Radiology Case Reports 20 (2025) 2544–2548

Available online at www.sciencedirect.com

ScienceDirect

journal homepage: www.elsevier.com/locate/radcr

Case Report

A case of multiple pancreatic metastases from renal cell carcinoma mimicking a neuroendocrine tumor ☆

Akina Miyamoto, MD[a,], Hiroyuki Kuroda, MD[a], Rika Yoshida, MD[a], Takeshi Yoshizako, MD[a], Yuko Makihara, MD[b], Hoshio Uwabe[c], Takashi Kishi, MD[d], Yasushi Kaji, MD, PhD[a]*

[a] *Department of Radiology, Shimane University Faculty of Medicine, Izumo, Japan*
[b] *Department of Radiology, Shimane Prefectural Central Hospital, Izumo, Japan*
[c] *Department of Radiology, Shimane University Hospital, Izumo, Japan*
[d] *Department of Digestive and General Surgery, Shimane University, Faculty of Medicine, Izumo, Japan*

ARTICLE INFO

Article history:
Received 28 September 2024
Revised 4 February 2025
Accepted 6 February 2025

Keywords:
Renal cell carcinoma
Somatostatin receptor scintigraphy
Neuroendocrine tumor
Pancreatic metastasis

ABSTRACT

Herein, we present the case of a 73-year-old man with recurrent pancreatic tumors 20 years postnephrectomy for clear cell renal cell carcinoma (RCC). Imaging studies revealed multiple hypervascular tumors in the pancreas, posing a diagnostic challenge in differentiating RCC metastases from well-differentiated neuroendocrine tumors (NETs). Magnetic resonance imaging (MRI) chemical shift imaging played a pivotal role in suggesting the presence of fat, supporting RCC metastasis. Surgical resection confirmed the diagnosis.

Introduction

Somatostatin receptor scintigraphy (SRS) is a standard diagnostic examination for pancreatic and gastrointestinal neuroendocrine tumors (NETs) [1]. However, the radiolabeled tracers used in SRS also exhibit uptake in other tumors with strong somatostatin receptor type 2 (SSTR2) expression, such as renal cell carcinoma (RCC) [2,3].

RCC contains fat, with clear cell RCC notably having a relatively high prevalence of fat content [4].

In this report, we present a case of pancreatic metastasis from RCC that was challenging to distinguish from pancreatic NETs using computed tomography (CT), SRS, and fluorodeoxyglucose-positron emission tomography/computed tomography (FDG-PET/CT). However, chemical shift imaging using magnetic resonance imaging (MRI) was found to be useful for diagnosis.

☆ Competing Interests: The authors declare that they have no known competing financial interests or personal relationships that could have appeared to influence the work reported in this paper.

* Corresponding author.
E-mail address: amymt@med.shimane-u.ac.jp (A. Miyamoto).

https://doi.org/10.1016/j.radcr.2025.02.024

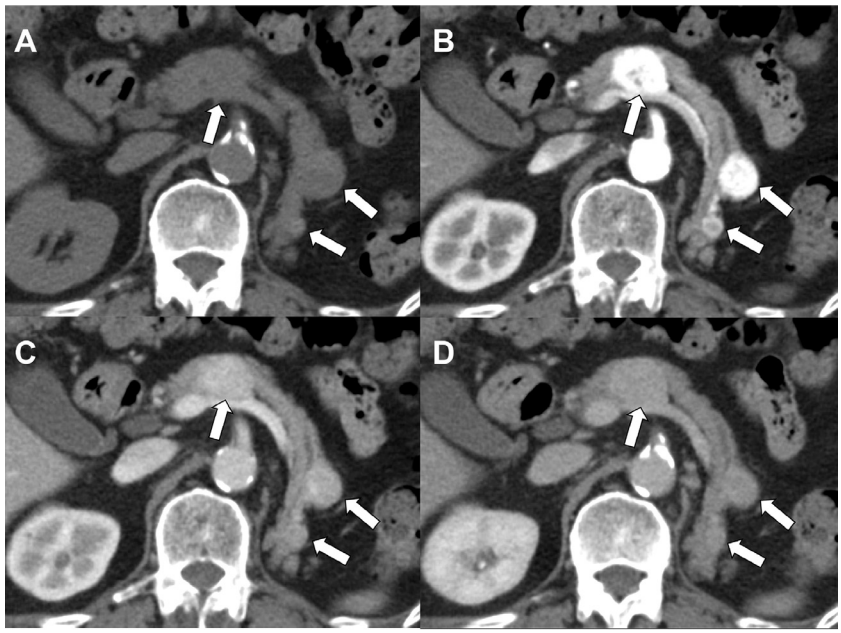

Fig. 1 – Computed tomography (CT). (A) Non–contrast-enhanced CT, (B) Contrast-enhanced CT, early arterial phase, (C) Contrast-enhanced CT, late arterial phase, (D) Contrast-enhanced CT, delayed phase.
The CT scans reveal multiple well-defined circular hypervascular tumors, each measuring less than 30 mm in diameter, distributed throughout the pancreas (arrows).

Case report

Twenty years post-left nephrectomy for clear cell RCC, a 73-year-old man presented to the orthopedic department of our hospital with numbness in his lower extremities. However, multiple pancreatic tumors were detected incidentally on CT scan in preparation for lumbar spine surgery.

His medical history included hypertension, dyslipidemia, hyperuricemia, gastroesophageal reflux disease, and cerebral infarction. His surgical history included left nephrectomy for clear cell RCC 20 years ago at another hospital, with postoperative follow-up having been completed; lumbar spinal stenosis 27 years ago; appendectomy; and carpal tunnel syndrome. The family history is unknown.

Physical examination revealed no back or abdominal pain, except for left lower abdominal pain.

Blood tests revealed that the serum levels of tumor markers, carcinoembryonic antigen (CEA), and carbohydrate antigen 19-9 (CA19-9), were within normal ranges. Results of the blood tests, including complete blood count and laboratory blood biochemistry, were normal.

Contrast-enhanced CT revealed four well-defined hypervascular circular tumors measuring less than 30 mm in diameter throughout the pancreas (Fig. 1). The tumors showed mild high signal intensity on T2-weighted imaging (WI), high signal intensity on diffusion-weighted imaging, and a reduction in the apparent diffusion coefficient (0.63×10^{-3} mm^2/s, $b = 800$ s/mm^2) during the MRI examination. The tumors exhibited a reduction in signal intensity from in-phase to opposed-phase T1-WI, indicating the presence of fat (Fig. 2). FDG-PET/CT revealed low FDG uptake in the tumors, with a maximum standardized uptake value (SUVmax) of 2.6 (Fig. 3). No other lesions indicating metastasis were identified. Accumulation of indium-111-labeled pentetreotide was observed in multiple pancreatic tumors on SRS (Fig. 4).

Based on the patient's imaging findings and relevant history, RCC metastasis to the pancreas was suspected to be more likely than well-differentiated NETs; therefore, the pancreas was resected.

Macroscopically, yellow-brown tumors with internal hemorrhage were observed. Hematoxylin and eosin (H&E)-stained images showed cells with pale-to-eosinophilic granular cytoplasm, and immunohistochemistry revealed positivity for CD10 and partial positivity for PAX8, leading to the diagnosis of pancreatic metastasis from clear cell RCC.

Discussion

RCC is usually hematogenous, and the common sites of metastasis are the lungs, liver, and bones. Pancreatic metastasis accounts for approximately 2.8% of all RCC metastases [5]. Conversely, RCC is the most common primary site of metastatic pancreatic tumors (70.5%) [6]. RCC is known to selectively metastasize to the pancreas, possibly due to the "seed and soil" mechanism proposed by Paget, wherein tumor cell adhesion, growth, and metastasis formation occur selectively in organs where host and tumor cell characteristics precisely match [7,8]. Pancreatic RCC metastasis is often a late recurrence, with an average recurrence interval of more than 10 years and a maximum reported duration of 32 years [9]. Although metastatic pancreatic tumors are rare among pancreatic malignancies (approximately 2%-5%)

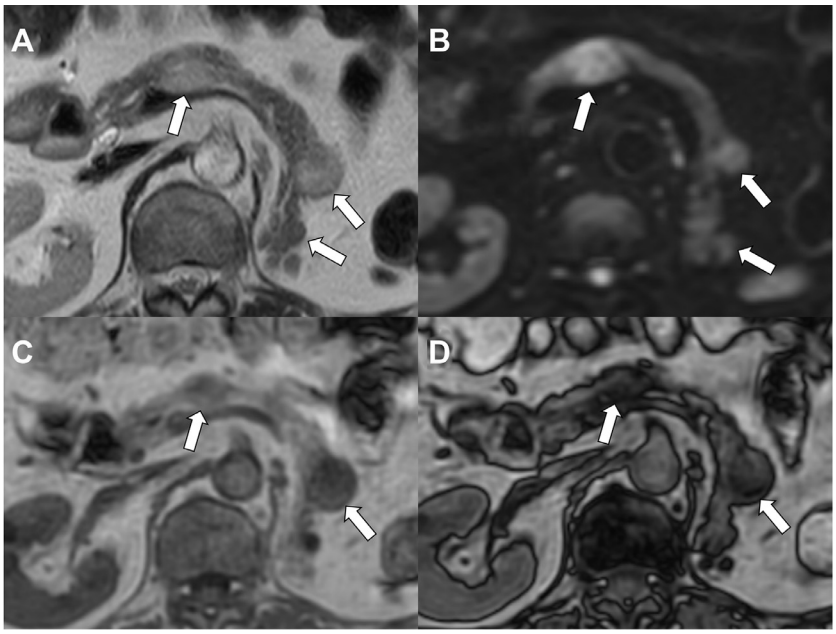

Fig. 2 – Magnetic resonance imaging (MRI). (A) T2-weighted image (T2WI), (B) Diffusion-weighted image (DWI), (C) In-phase of T1-weighted image (T1WI), (D) Opposed-phase of T1WI. Pancreatic tumors show mild high signal intensity on T2WI and high signal intensity on DWI. They exhibit reduced signal intensity from in-phase to opposed-phase T1WI, indicating the presence of fat (arrows).

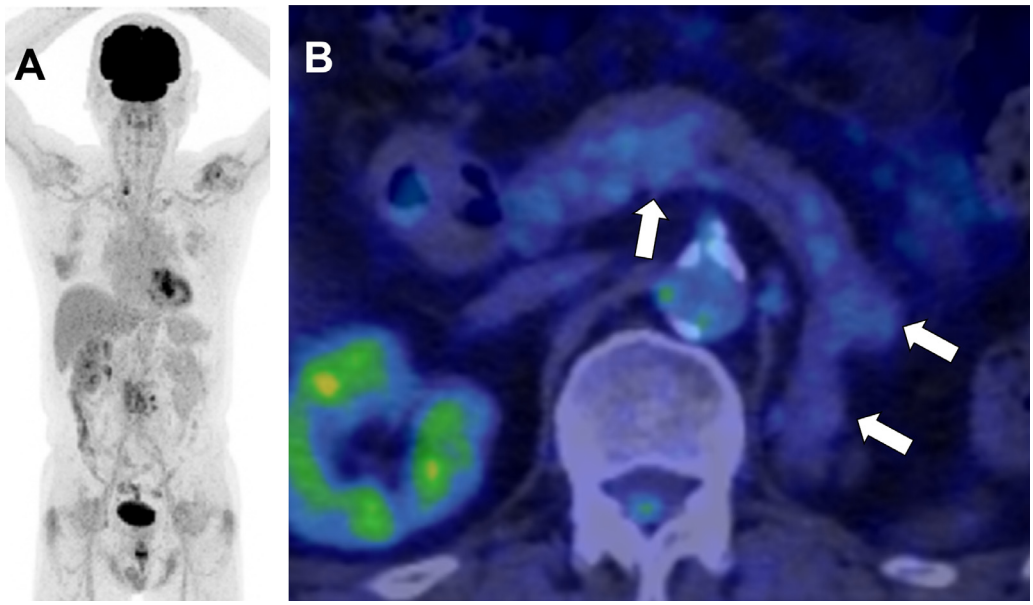

Fig. 3 – Fluorodeoxyglucose-positron emission tomography/computed tomography (FDG-PET/CT). (A) 3D-MIP image, (B) FDG-PET/CT image. FDG-PET/CT shows low FDG uptake in pancreatic tumors with a maximum standardized uptake value (SUVmax) of 2.6 (arrows).

[9], patients with a history of RCC should be suspected of pancreatic RCC metastasis even after a long postoperative period.

SRS performed after the initial suspicion of pancreatic NETs revealed a significant accumulation of pancreatic metastases from RCC. Although SRS is commonly used for the diagnosis and staging of pancreatic and gastrointestinal NETs [1], somatostatin receptors (SSTRs) are not specific to NETs, as they are also expressed in tumors such as RCC, paragangliomas, pituitary tumors, small cell lung cancer, and meningiomas [2]. The frequency of SSTR expression in RCC is high (72%), with SSTR2 being predominantly expressed

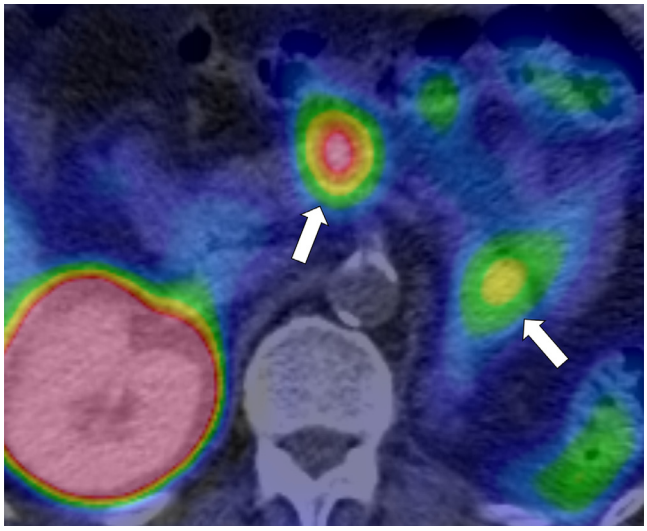

Fig. 4 – Somatostatin receptor scintigraphy (SRS). Fusion image after the 24-hour phase. SRS reveals the accumulation of Indium-111-labeled pentetreotide in multiple pancreatic tumors (arrows).

[2,10]. Several reports have identified recurrent or metastatic lesions, including pancreatic metastases from RCC, using ^{68}Ga-labeled 1,4,7,10-tetraazacyclododecane-N,N′,N″,N‴-tetraacetic acid-D-Phe^{1}-Tyr^{3}-octreotate (DOTATATE) -PET/CT or ^{68}Ga-labeled 1,4,7,10-tetraazacyclododecane-N,N′,N″,N‴-tetraacetic acid-D-Phe^{1}-Tyr^{3}-octreotide (DOTATOC) -PET/CT [11,12], and SSTR expression has been observed in RCC metastases [13,14]. It is presumed that SSTR was expressed in the tumors in our case. Therefore, SRS accumulation is not specific to NETs.

RCC is known for its low FDG uptake, and low detection sensitivity for postoperative recurrence (74%) [15]. The accumulation patterns on SRS and FDG-PET/CT in RCC pancreatic metastases may be similar to those in well-differentiated pancreatic NETs, indicating the limited utility of these modalities in distinguishing between the two.

RCC is known to contain fat, with reported rates of fat detection using MRI chemical shift imaging being 64%-73% for clear cell RCC, 17%-29% for papillary RCC, and 9%–13% for chromophobe RCC [4]. Conversely, fat-containing pancreatic NETs have also been reported, with a fat detection rate of 23.5% using chemical shift imaging [16]. Fat-rich pancreatic NETs are more prevalent in von Hippel–Lindau disease [17] and multiple endocrine neoplasia type 1 (MEN1) syndrome [18]; however, they are also found in 34.6% of NETs without a family history [16]. Fat content is a characteristic of RCC, particularly clear cell RCC; however, it is not specific. Therefore, differentiating between RCC and NETs based solely on the presence of fat should be performed carefully.

Conclusion

Herein, we report the case of a patient with multiple pancreatic metastases of RCC with SRS accumulation. This case underscores the importance of considering pancreatic RCC metastases in patients with a history of RCC, even after a long disease-free interval. MRI chemical shift imaging is a valuable tool in differentiating fat-containing pancreatic tumors. However, because NETs with abundant fat variants exist, distinguishing them based on imaging alone is challenging.

Patient consent

Informed consent was obtained from the patient.

REFERENCES

[1] Krenning EP, Bakker WH, Kooij PP, Breeman WA, Oei HY, de Jong M, et al. Somatostatin receptor scintigraphy with indium-111-DTPA-D-phe-1-octreotide in man: metabolism, dosimetry and comparison with iodine-123-tyr-3-octreotide. J Nucl Med 1992;33(5):652–8. https://jnm.snmjournals.org/content/33/5/652.

[2] Reubi JC, Waser B, Schaer JC, Laissue JA. Somatostatin receptor sst1-sst5 expression in normal and neoplastic human tissues using receptor autoradiography with subtype-selective ligands. Eur J Nucl Med 2001;28(7):836–46. doi:10.1007/s002590100541.

[3] Kwekkeboom DJ, Krenning EP, Scheidhauer K, Lewington V, Lebtahi R, Grossman A, et al. ENETS consensus guidelines for the standards of care in neuroendocrine tumors: somatostatin receptor imaging with 111In-pentetreotide. Neuroendocrinology 2009;90(2):184–9. doi:10.1159/000225946.

[4] Karlo CA, Donati OF, Burger IA, Zheng J, Moskowitz CS, Hricak H, et al. MR imaging of renal cortical tumours: qualitative and quantitative chemical shift imaging parameters. Eur Radiol 2013;23(6):1738–44. doi:10.1007/s00330-012-2758-x.

[5] Klugo RC, Detmers M, Stiles RE, Talley RW, Cerny JC. Aggressive versus conservative management of stage IV renal cell carcinoma. J Urol 1977;118(2):244–6. doi:10.1016/S0022-5347(17)57959-8.

[6] Sweeney AD, Wu MF, Hilsenbeck SG, Brunicardi FC, Fisher WE. Value of pancreatic resection for cancer metastatic to the pancreas. J Surg Res 2009;156(2):189–98. doi:10.1016/j.jss.2009.01.017.

[7] Paget S. The distribution of secondary growths in cancer of the breast. Lancet 1889;133(3421):571–3. doi:10.1016/S0140-6736(00)49915-0.

[8] Sellner F, Thalhammer S, Klimpfinger M. Isolated pancreatic metastases of renal cell carcinoma—clinical particularities and seed and soil hypothesis. Cancers 2023;15(2):339. doi:10.3390/cancers15020339.

[9] Ballarin R, Spaggiari M, Cautero N, De Ruvo N, Montalti R, Longo C, et al. Pancreatic metastases from renal cell carcinoma: the state of the art. World J Gastroenterol 2011;17(43):4747–56. doi:10.3748/wjg.v17.i43.4747.

[10] Reubi JC, Kvols L. Somatostatin receptors in human renal cell carcinomas. Cancer Res 1992;52(21):6074–8. https://aacrjournals.org/cancerres/article/52/21/6074/498269/Somatostatin-Receptors-in-Human-Renal-Cell.

[11] Vamadevan S, Le K, Shen L, Loh H, Mansberg R. 68Ga-DOTATATE uptake in solitary pancreatic metastasis from clear cell renal cancer. Clin Nucl Med 2017;42(9):700–1. doi:10.1097/RLU.0000000000001765.

[12] Nakamoto Y, Ishimori T, Shimizu Y, Sano K, Togashi K. Clinical utility of ^{68}Ga-DOTATOC positron emission tomography/computed tomography for recurrent renal cell carcinoma. Eur J Nucl Med Mol Imaging 2019;46(7):1524–30. doi:10.1007/s00259-019-04298-4.
[13] Peter L, Sänger J, Hommann M, Baum RP, Kaemmerer D. Molecular imaging of late somatostatin receptor-positive metastases of renal cell carcinoma in the pancreas by 68Ga DOTATOC PET/CT: a rare differential diagnosis to multiple primary pancreatic neuroendocrine tumors. Clin Nucl Med 2014;39(8):713–16. doi:10.1097/RLU.0000000000000351.
[14] Höög A, Kjellman M, Mattsson P, Juhlin CC, Shabo I. Somatostatin receptor expression in renal cell carcinoma: a new front in the diagnostics and treatment of renal cell carcinoma. Clin Genitourin Cancer 2018;16(3):e517–20. doi:10.1016/j.clgc.2018.03.011.
[15] Alongi P, Picchio M, Zattoni F, Spallino M, Gianolli L, Saladini G, et al. Recurrent renal cell carcinoma: clinical and prognostic value of FDG PET/CT. Eur J Nucl Med Mol Imaging 2016;43(3):464–73. doi:10.1007/s00259-015-3159-6.
[16] Fukukua Y, Shindo T, Higashi M, Takumi K, Umanodan T, Yoneyama T, et al. Computed tomography and magnetic resonance imaging features of lipid-rich neuroendocrine tumors of the pancreas. World J Gastroenterol 2015;21(34):10008–17. doi:10.3748/wjg.v21.i34.10008.
[17] Lubensky IA, Pack S, Ault D, Vortmeyer AO, Libutti SK, Choyke PL, et al. Multiple neuroendocrine tumors of the pancreas in von Hippel-Lindau disease patients: histopathological and molecular genetic analysis. Am J Pathol 1998;153(1):223–31. doi:10.1016/S0002-9440(10)65563-0.
[18] Fryer E, Serra S, Chetty R. Lipid-rich ("clear cell") neuroendocrine tumors of the pancreas in MEN I patients. Endocr Pathol 2012;23(4):243–6. doi:10.1007/s12022-012-9221-z.